Activity Monitoring with Airborne SAR Imagery

Hélène Oriot
ONERA - The French Aerospace Lab
F-91761 Palaiseau
France

helene.oriot@onera.fr

ABSTRACT

One of the main advantages of Radar sensors is that they are active sensors thus producing measurements almost independent from weather conditions. Airborne or spaceborne radars, used for ground imaging in a Synthetic Aperture Radar (SAR) mode, ally this advantage with high resolution capabilities. SAR imaging is therefore an appropriate tool for ground surveillance and activity monitoring. This papers aims at providing insights to understand the different kinds of changes that can be detected with airborne imagery in various conditions (UHF, L, X band, mono polarisation or full polarisation modes) and to give methods to implement such algorithms.

1.0 INTRODUCTION

SAR imagery is indeed almost independent of weather conditions since, theoretically, two images obtained, in the same mode but at different time, with a sensor following each time the exact same path, are identical both in amplitude and phase. Reciprocally, if two images acquired under the above mentioned conditions are not identical, it implies that a change occurred on the ground between the two acquisitions dates.

Different types of changes may be observed in SAR imagery:

1) Changes due to the presence of man-made objects (such as vehicles [1], mines [2] ...). These changes are localised and one can consider that only a few of them are present in a SAR image. These changes are usually analysed using two images, a reference image and a test image. Several authors have studied these kinds of changes mostly based on airborne images at different bands (from UHF for concealed vehicles [1], to X and Ku band images).
2) Changes of the ground linked to human activity (footprints tracks, object burial) [3]. These changes are also localised but can have a linear extent. As above, these changes are detected using two images. Because they correspond to small size phenomena, they are usually detected on high or very high resolution SAR images, with airborne radar [4], but also spaceborne radar such as Cosmo-Skymed (*http://www.e-geos.it/news/e-GEOS%20geoint.pdf*).
3) Changes due to natural events (flooding events, ...), natural evolution (crop monitoring, ...) [5] or urban construction [6]. These changes are generally analysed from spaceborne sensors with medium or low resolution but large extent capabilities using the repeatability of satellite SAR imagery. A lot of work has been done on the optimal use of stack of radar images to monitor these kinds of changes, in C, L or X band.

Here we restrain ourselves to the study of the former two kinds of changes which correspond to the problematic of surveillance using two (change detection) or more images (activity monitoring).

In order to get an insight of the physical observables, let's analyse a ground area corresponding to a resolution cell size on a SAR image. The simplest model is considering that the complex backscattered signal is the coherent sum of a large number of elementary scatterers randomly distributed within the

resolution cell. A resolution cell located nearby and composed of different backscatterers of the same nature presents a different amplitude and phase. It can be shown [7] that the amplitude of the resolution cell is a random variable with a Rayleigh distribution, whereas the phase presents an uniform distribution.

Suppose that the same ground area is imaged twice under exactly the same conditions and let's compare the amplitude and phase of the two SAR signals:

- If no change has occurred on the ground, the elementary scatterers of the resolution cell remain exactly at the same position so that the coherent summation is the same in amplitude and phase as at the first date.
- If the nature of the ground has not changed between the two acquisition dates but the elementary scatterers have been displaced (for example let's consider a dirt road and a car that drove along it at a time in between the two acquisition dates so that small rocks were displaced), the resolution cell radiometry still follows the same Rayleigh distribution but theresolution cell phase changed. This kind of change is called "coherent change" and its studying is known as "Coherent Change Detection (CCD) techniques [4].
- If the nature of the ground changed (apparition of an object such as a car or a building, deforestation ...), the radiometry of the resolution cell does not follow the same statistical law anymore and the image phase changes. This kind of changes are named "incoherent changes" since they can be detected without analysing the phase of the SAR images.

The main difference between coherent changes and incoherent changes is that incoherent changes correspond to phenomena that are present in one image and not in the other: a car is parked along a road in the first image and is not there anymore in the second one (see example on Figure 1, left) or a field has grown from one image to the other. Coherent changes correspond to phenomena that have occurred in between the two acquisition dates. A car may have crossed the scene at a date in between the two acquisition dates so that the ground has slightly changed. At the time of the second image, the car is not in the image anymore but the track can be seen. This technique allows detecting activity that occurred in the time interval (see example on Figure 1, right)

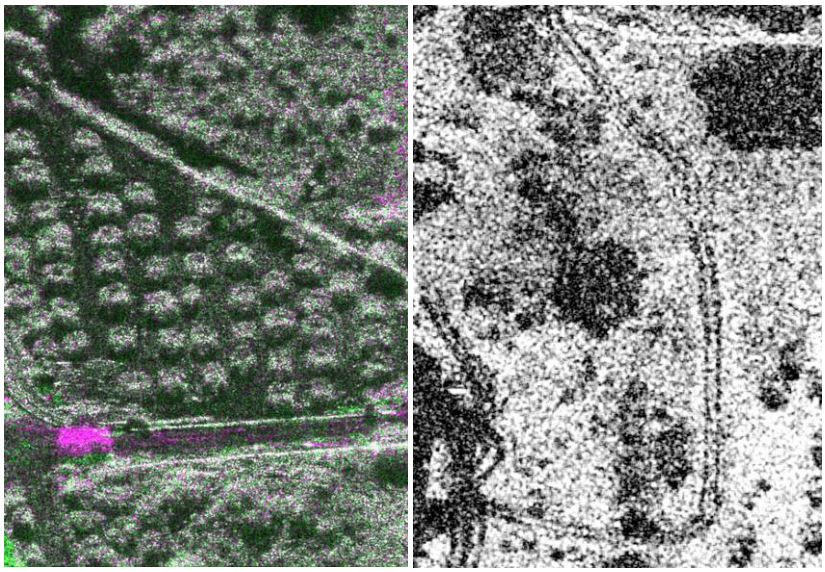

Figure 1: Left: colour composite of two amplitude images acquired at different times on the same area (X band data). The magenta area corresponds to car arrival. Right: car track signature on a coherence image.

In reality images do not always satisfy the hypotheses mentioned above:

- The two sensor trajectories may not be identical leading to different geometries: the resolution cell does not correspond to the same area on the ground in the two images. Because of that, a matching procedure is used to superimpose the two images precisely. Then, we will see that there is an upper limit on the distance between the two trajectories beyond which coherent change detectors are inefficient.
- The SAR images are corrupted by thermal noise so that even if two images are taken from exactly the same trajectory, the amplitudes and phases of a resolution cell may differ
- The radiometry of the images cannot always be modeled by a Rayleigh distribution.
- Changes other than those of interest may induce amplitude or phase changes leading to false alarms.

Therefore, change detection techniques must be robust to cope with these problems.

In the following section we will present the notations used in this paper, then we will explain the geometrical constraints linked to change detection algorithms. In section #4 we will explain image matching procedures so that the two images are precisely superimposed. In section #5 the main methods for detecting changes using only two images will be presented, then section #6 will be dedicated to the activity monitoring problem using more than two images.

2.0 NOTATIONS

The following notations will be used in the paper:

- $x_{i,j}$ is the complex radiometry of pixel (i,j) of interest of the first image, $y_{i,j}$ is the same pixel complex radiometry in the second image. The i-or y axis- corresponds to the along track direction, the j -or x axis-, corresponds to the range direction.
- when the two images are not in the same geometry: let (i,j) be a pixel of the first image and (i',j') the corresponding pixel in the second image. We call disparity images the two following images:
  - range disparity image: gives the value $\delta j = j'-j$, for each pixel (i,j) of the first image
  - azimuth disparity image: gives $\delta i=i'-i$ for each pixel (i,j) of the first image
- x* stands for the complex conjugate of x
- λ is the wavelength associated with the central frequency of the emitted wave.
- θ is the incident angle of the wave
- For the sake of simplicity, the pixels of a rectangular windows of size (2n+1)x(2n+1) pixels centered on pixel (i,j) which should be named $\boldsymbol{x}_{i+m,j+l}$ with $-\boldsymbol{n} \leq \boldsymbol{m} \leq \boldsymbol{n}$ and $-\boldsymbol{n} \leq \boldsymbol{l} \leq \boldsymbol{n}$, will be named $\boldsymbol{x}_{\boldsymbol{k}}$ with $\mathbf{1} \leq \boldsymbol{k} \leq \boldsymbol{N}$ and $N=(2n+1)^2$
- $\mathbf{X}$ represents a vector, $\mathbf{X}^{\mathbf{H}}$ represents the complex conjugate transpose of $\mathbf{X}$

3.0 GEOMETRICAL CONSTRAINTS

As mentioned in the latest section, change detection techniques are based on the fact that a same resolution cell gives a radar output with the same phase and amplitude if imaged twice under the same line of sight.

3.1 incoherent change detection

Incoherent change detection algorithms are based on the comparison of the statistical laws of the two images. The better the similarity between the two statistical laws, the better the result. To our knowledge there is no theoretical results on the dependency of the statistical distribution of the amplitude images with incidence or heading angles but this dependency exists (for example, the clutter mean intensity changes with incidence [8]). Therefore, one would prefer to have images with the same line of sight to remove effects of difference of incidence or heading between the two acquisitions.

Furthermore, in presence of relief (urban area or hilly area), the image is affected by the well known foreshortening effect [9] which depends on incidence: If the two incidences differ, a same resolution cell does not correspond to the same part of the ground so the amplitude statistical law may differ.

Finally, there is no true geometrical constraint for incoherent change detection techniques but the closest the two lines of sight are, the better.

3.2 coherent change detection

In coherent change detection, the problematic is slightly different since the signal phases are compared. When the speckle is fully developed, the spatial phase distribution is uniform between [0 2π], but the phase difference of two images with close line of sights is not uniformly distributed anymore and carries information. This is the principle of SAR interferometry. It has been shown [10] and [11] that, only the common spectra expressed in the same coordinate system of the two images interfer.

- First the images must have been acquired and processed with a common doppler bandwidth as explained on Figure 2. That means that only signals acquired with a same squint angle[1] will interfer. The interferometric azimuth resolution is the resolution obtained by this common doppler bandwidth. This constraint is generally achievable as soon as the azimuthal antenna pattern is large enough to compensate airborne heading uncertainties and the processing procedure is performed accordingly.

- Then, in order to respect the spectral constraint in the range direction, the difference of incidence angles between the two trajectories must satisfy:

$$|\delta\theta| \leq \frac{\lambda \tan(\theta - \beta)}{2.range\_resolution} \quad (1)$$

β being the slope of the imaged terrain

In case of volumic backscattering (for example propagation through the forest in L and P band), one can consider that the above condition must be true for both β=0 and β=π/2. In fact, depending on the frequency and on the attenuation of the wave propagating through the volume, the model may be refined and this condition may be slightly loosened [12].

[1] the squint angle is defined as the angle between the velocity vector of the first image and the line of sight

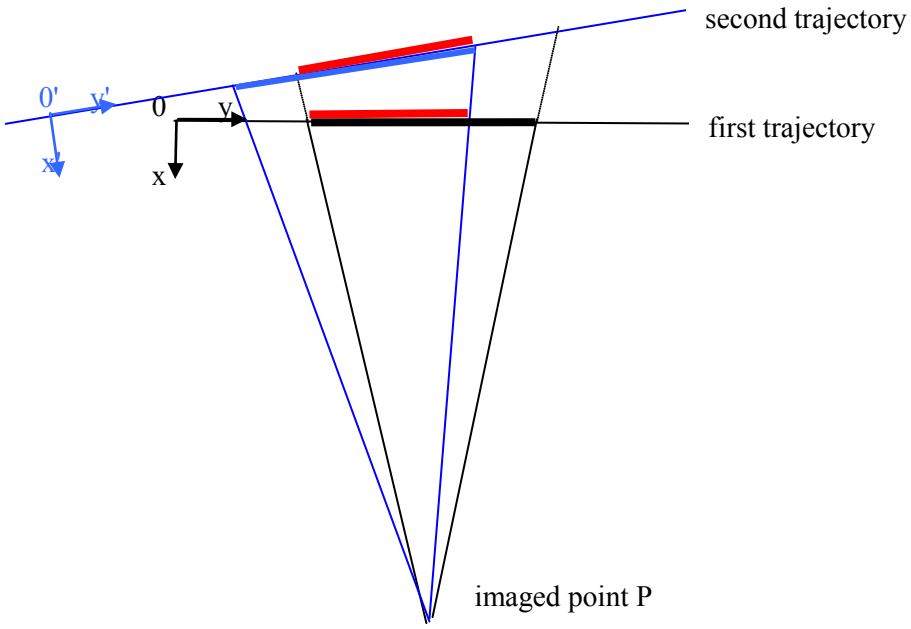

Figure 2: View from above of two trajectories (one in blue, the second in black). The two integration intervals are indicated in bold and the common integration interval is indicated in red bold.

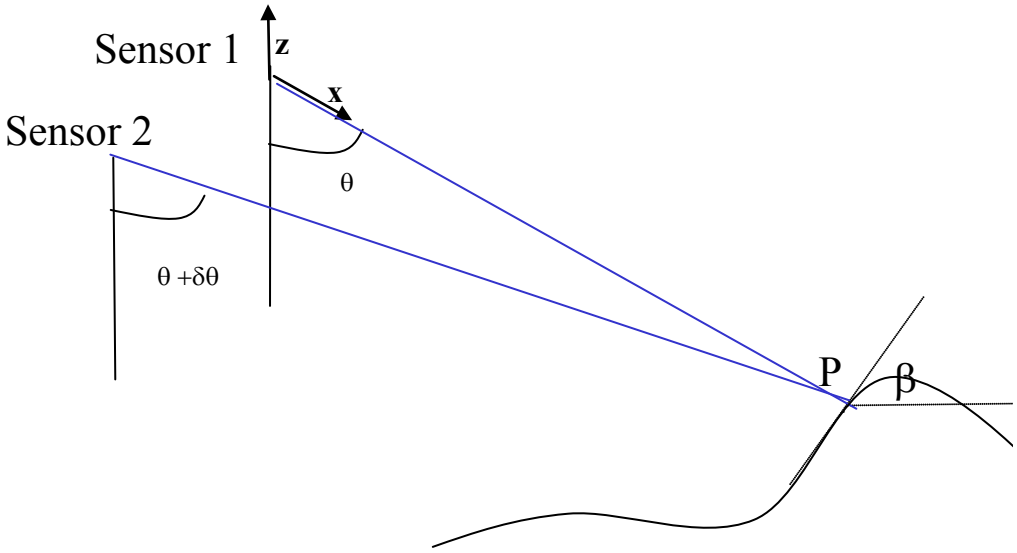

Figure 3: View of the acquisition geometry in the plane perpendicular to the first trajectory velocity vector.

In order to lower the noise on coherence images, the two spectra are trimmed to keep only the common spectra of the two images with the consequence of degrading the resolution of the output images.

Equation (1) shows that the interferometric condition is more demanding in term of flight control for high frequency, low resolution images and short range images. For example, if we consider a X-band system, 30cm slant range resolution with a 20° depression angle at a range of 20 km, the two trajectories should not

be more than 2700 m away in order to be in interferometric conditions. Furthermore, if one wants to have a 60cm resolution coherence image, the two trajectories must be less than 1300m away.

Finally, coherent change detection is possible only for trajectories satisfying eq (1) but better results are expected for nearby trajectories (better interferometric spatial resolution).

4.0 IMAGE CO-REGISTRATION

Image co registration is an important step of change detection in SAR imagery. Generally, the procedure is not completely described in literature and each team has its own methodology. The methodology highly depends on the kind of SAR image used, either spaceborne or airborne, on resolution and on the accuracy of the geometrical model of the SAR data (this geometrical model generally depends on the SAR processor). Generally speaking image co-registration is performed in three steps; each of them may be skipped depending on the SAR data.

1. co-registration based on the geometrical model of the SAR data
2. image matching, matches selection and interpolation
3. co-registration based on the disparity map

In the first step, each pixel from one image is projected on the second image thanks to the radar equations. A Digital Elevation Model (DEM) of the area may be needed in order to have an accurate result.

The resampling procedure is then performed using a phase preserving interpolation (especially for CCD techniques or polarimetric change detection) so that the phase of the resampled image is not corrupted.

In presence of unknown relief, or if the sensor trajectories are not known with a good accuracy, the first step may not be sufficient to obtain a pixel or sub-pixel co-registration accuracy. In this case, a second step is applied: the images are matched together in order to estimate residual two dimensional displacements, then one image is resampled in the geometry of the other one.

The output disparity maps (images of $\delta i=i'-i$ and $\delta j=j'-j$ for i', j' maximising a correlation criterion) are generally noisy and have to be filtered before being used for resampling. Usually a selection procedure based on the shape of the correlation criterion [13] gets rid of poor matches.

The sparse disparity maps are then interpolated. In airborne SAR imagery, these disparity maps depends on the trajectory errors which can be modeled as a smooth function in range and azimuth (except for very high resolution images for which they may be a dependency of the range disparity map with altitude). Details of such techniques may be found in [14]

Figure 4: Example of two disparity maps (range (middle image) and azimut (right image)) obtained on UHF band data from the SETHI sensor of ONERA on the Paracou dataset (left image) [15]. The two disparity images are scaled from -0.5 pixels (black) to +0.5 pixels

Once the images are co-registered, a colour composite of the two amplitude image can rapidly give a clue of changes and the computation of the local coherency gives very quickly an insight of coherent changes as shown in Figure 1.

5. TWO IMAGES CHANGE DETECTION

5.1 Incoherent change detection

In the following we will suppose that we have two coregistered images. Generally speaking, the coregistration accuracy should be pixellic for incoherent change detection.

5.1.1 Mono polarisation

Let's consider a small area of the first image (square of 5x5 pixels for example) to be compared to the same area in the second image. Under the hypothesis of circular complex gaussian clutter, it can be shown that the Generalised likelihood ratio test leads to the following test, called ratio test [23],[16]

$$z_{CD} = \frac{\sum_{1}^{N} |y_k|^2}{\sum_{1}^{N} |x_k|^2} \quad \text{if } z_{CD}>T \text{ there is an arrival, if } z_{CD}<1/T \text{ there is a departure} \tag{2}$$

This test is CFAR (constant false alarm rate) under the hypothesis that in case there is no change, the clutters of image#1 and image #2 have exactly the same statistical distribution. z_{CD} is a Fisher distribution and T can be chosen for a given false alarm probability.

In reality, for airborne SAR systems, the calibration procedure may not be accurate enough and the two images may differ by an unknown factor. In order to encompass this problem, detection techniques may be used on the ratio image: The ratio of the test zone is compared to the ratio of an area surrounding the test zone which is supposed to be unchanged.

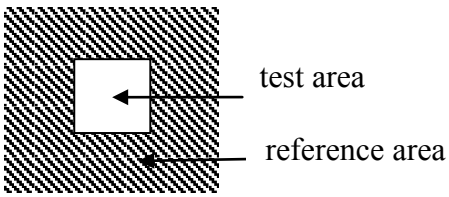

Figure 5: Definition of the test area and the reference area.

$$z_{CD'} = \frac{Z_{CD}(\text{test area})}{z_{CD}(\text{reference area})} \tag{3}$$

Other criteria may also be found in literature [2],[17]. Some are dedicated to low frequency SAR [1]

Figure 6 presents an example of change detection applied to X band 20cm resolution airborne SAR data.

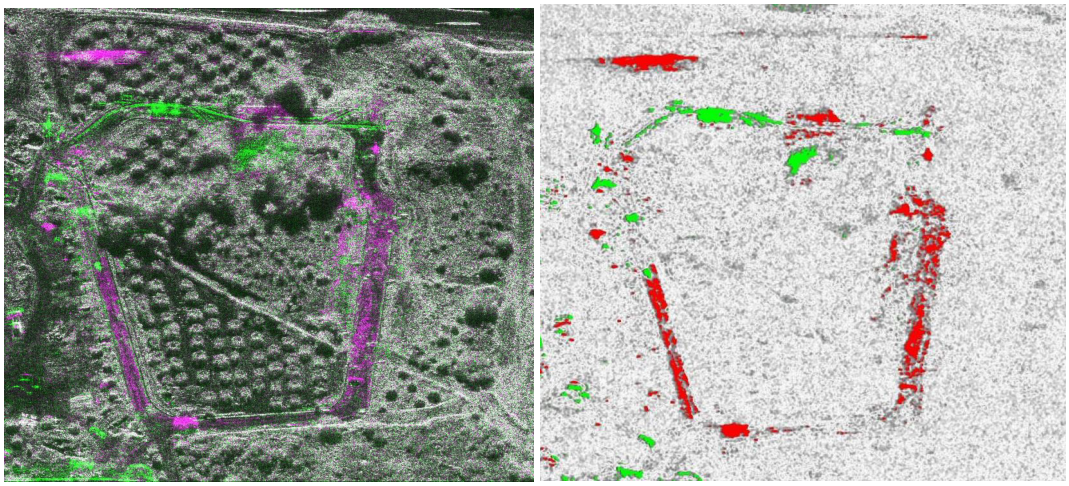

Figure 6: Left image: colour composite of two images (X band data). Right image: ratio image with detected changes; the green ones correspond to departures and the red ones to arrivals.

5.1.2 Full polarisation

In case of fully polarised data, the clutter is still modeled by a random complex circular gaussian variable and the two images are compared using their covariance matrices.

The full polarised dataset is modelled as a vector of 3 dimensions corresponding to the three acquired channels: HH (horizontal transmitted wave and horizontal received wave), HV (horizontal transmitted wave and vertical received wave and Vv (Vertical transmitted wave and vertical received wave)

$\boldsymbol{X} = \begin{bmatrix} \boldsymbol{x}_{HH} \\ \boldsymbol{x}_{HV} \\ \boldsymbol{x}_{VV} \end{bmatrix}$, with x_{HH}, x_{HV}, x_{VV} being the complex data of the three SAR image HH, HV and VV.

X follows the probability density function:

$$p(\boldsymbol{X}|\boldsymbol{C}) = \frac{1}{\pi^3|\boldsymbol{C}|} e^{-X^H C^{-1} X} = \frac{1}{\pi^3|\boldsymbol{C}|} e^{-tr\left[C^{-1} X^H X\right]}, \tag{4}$$

C is the covariance matrix of the data vector X and |C| stands for the determinant of matrix C

Under the hypothesis of random complex circular gaussian clutter, it can be shown that the Generalised likelihood ratio test leads to the following test [16]:

$$z_{POLCD} = \frac{\left|\sum_1^N \boldsymbol{X}_i \boldsymbol{X}_i{}^H\right| \left|\sum_1^N \boldsymbol{Y}_i \boldsymbol{Y}_i{}^H\right|}{\frac{1}{2}\left(\left|\sum_1^N \boldsymbol{X}_i \boldsymbol{X}_i{}^H\right| + \left|\sum_1^N \boldsymbol{Y}_i \boldsymbol{Y}_i{}^H\right|\right)^2} \tag{5}$$

Here, only the determinants of the covariance matrix of each dataset are compared. It means that the incoherent polarimetric behaviours of the two datasets are compared. This criterion is therefore well fitted to fully developed speckle area. Nevertheless, interesting results are obtained on vehicles.

Here is an example on an experiment which took place in French Guyana in 2009 [15]. UHF and L full polarimetric data were acquired over a period of one month (12 acquisitions) and during one acquisition; three cars were parked under cover as shown on (Figure 7 left) as well as a corner reflector. An example of a polarimetric change detection map is presented in Figure 7 right. Two out of three cars are detected. One non cooperative target is also detected (green circle) [22]. The statistics of the z_{polcd} criterion are computed for the 11 change detection configurations. Results presented in Table 1 show that the targets responses of the change detection map are much higher than the surrounding clutter which is a very good result.

Table 1: change detection statistics for the detected targets.

Target	mean	std
Isuzu	16 dB	+/-0.75 dB
Master	16.5 dB	+/-0.7 dB
Non cooperative target	10dB	+/-0.5 dB
Corner reflector	6dB	+/-1.4 dB
Clutter	0 dB	+/-1.4 dB

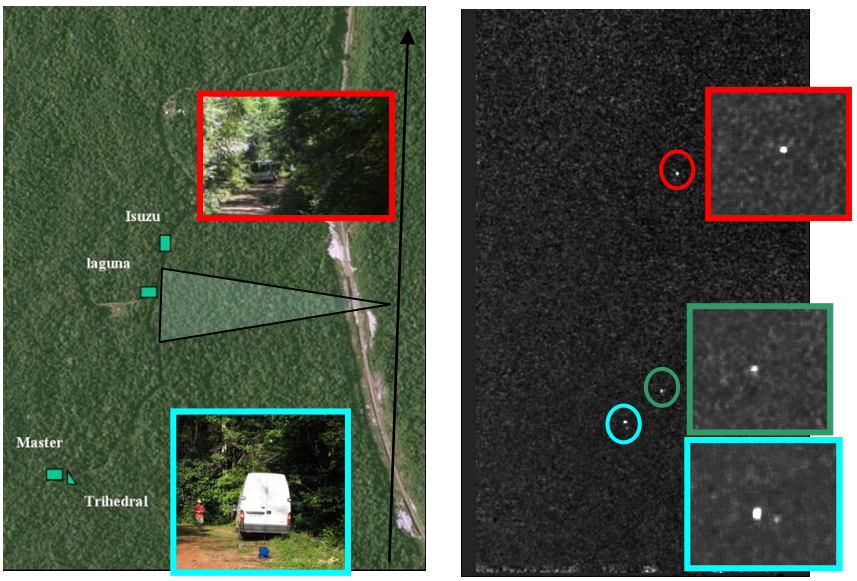

Figure 7: Left image: experiment setup Right image: polarimetric change detection results.

5.2 Coherent change detection

In the following we will suppose that we have two coregistered images. Generally speaking, the coregistration accuracy should be sub pixellic -of the order of 1/10th of a pixel - of coherent change detection.

5.2.1 Mono-polarisation

Coherent change detection is a technique that was developed with the arrival of high resolution imagery [4]. This technique detects subtle movement of the ground (small scatterers movements) that have happened in between the two acquisition dates and that cannot be distinguished on the amplitudes images.

The usual criterion is the coherence criterion (cf Eq 6) which tends towards 0 when the area has been modified and to one when the area has not changed.

$$coh = \left| \frac{\sum_{1}^{N} x_k y_k^*}{\sqrt{\sum_{1}^{N} |x_k|^2 \sum_{1}^{N} |y_k|^2}} \right| \tag{6}$$

L. Novak derived The Maximum Likelihood Estimator for change detection [16]: It leads to a slightly different criterion:

$$z_{CCD} = \frac{\left| \sum_{1}^{N} x_k y_k^* \right|}{\frac{1}{2}\left(\sum_{1}^{N} |x_k|^2 + \sum_{1}^{N} |y_k|^2\right)} \tag{7}$$

Changes occur for *coh* or z_{ccd} close to 0.

Additional criteria may be found in [18]. A Generalised Likelihood Ratio Test was also derived [14] and its implementation explained in [3].

Figure 8 shows an example of tracks visualisation through CCD. The tracks that are visible in the coherence image and z_{ccd} images are not detected on the z_{cd} image (cf Figure 6) or even seen on the colour composite image. The comparison of the z_{ccd} image and the coherence image shows the same behaviour.

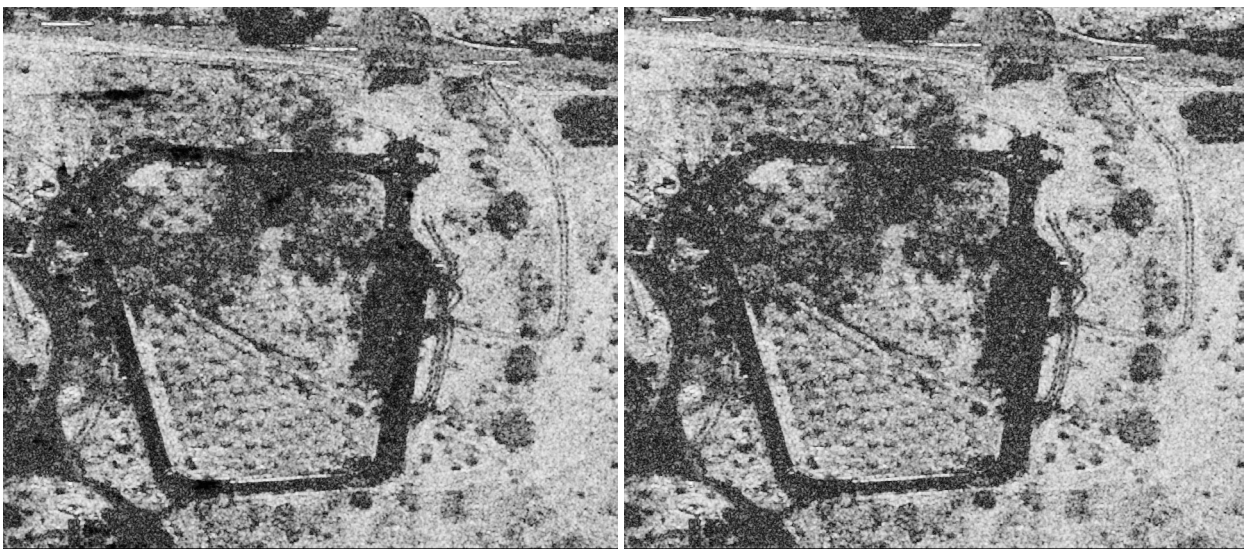

Figure 8: Left: Coherence image of the same area as Figure 6. Right: Corresponding Zccd image.

This technique is very powerful but has some limitations. Changes are observed by comparison with the surrounding. If the surrounding presents a low coherence level, tracks cannot be detected.

The difficulty is to predict which area is suitable for such a technique - that is what kind of clutter presents high coherence values. The answer is not straightforward: several phenomena have to be considered:

- First the coherence level of an unchanged area depends on its Clutter to Noise ratio (CNR) according to the relationship:

$$coh = \frac{CNR}{1 + CNR} \tag{8}$$

  Shadow areas have a zero coherence level and low backscattering areas (lakes, roads, or grass for low frequency radars) have low coherence levels. These kinds of surfaces are not suitable for CCD techniques.

- Coherence loss may be geometrical: as mentioned in [10] only the common spectrum of the two images are correlated so one has to trim the common spectrum in order to minimise the interferometric noise and enhance the coherence level in non changing areas

- Depending on the revisit time, temporal decorrelation may occur between the two images. Roughly speaking, the smaller the wavelength, the shorter the coherence time. Good results have been obtained in X band for time intervals of the order of 1 to 8 days (the example on figure 8 was acquired with a 2 day interval in south of France). In UHF or L band, one can use much longer time intervals. The coherence maps presented in figure 9 were computed with images acquired one week and two weeks apart over tropical forest. Good coherence level was reported [15] in UHF over periods of one month in tropical forest. Some natural surfaces decorrelates very quickly: At X band, forest decorrelates for time interval smaller than 5 seconds, and water decorrelates for a time interval smaller than one millisecond. Depending on the weather (rainy event or strong wind) grass, sand, crops may also decorrelates.

Figure 8 presents another example of CCD technique. Here, two coherence images (UHF band images) of a same area are presented. The above image corresponds to the amplitude image of the area. In the middle, a reference coherence image is displayed. The decorrelated parts correspond to low backscattering areas such as the river crossing the image. In the lower image, the decorrelated part is larger and corresponds to the presence of water or humidity under the forest in the vicinity of the river. That means that the CCD techniques successfully detected an under cover flooding area.

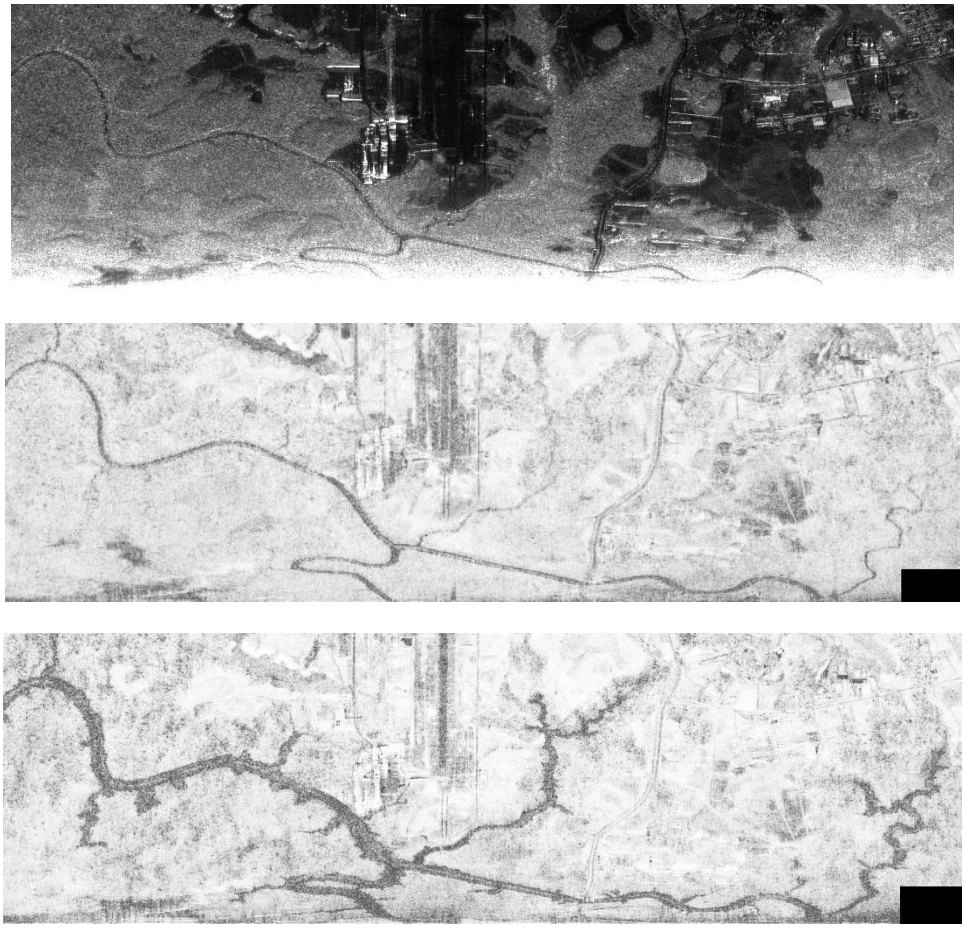

Figure 9: Above: SAR image of tropical forest with a river (UHF band, VV channel). Middle: Coherence image between two dates with no flooding event, Below coherence image between two dates with a flooding event on one of them.

5.2.2 Full polarisation

A field of on going research aims at modelling change detection criteria that measure the change of polarimetric behavior between the two acquisitions [19][20] in a coherent way.

6. MULTI -DATES CHANGE DETECTION

So far, we have presented different techniques to detect changes using a pair of images. In the framework of surveillance and activity monitoring it is interesting to update an activity map for each new available image.

The different criteria presented here can easily be written in a multi imaged framework as explained in [16], [21]. For example the POLCD criterion is written for 3 images (X, Y, Z) with the first two images being the references images [16].

$$\frac{\frac{1}{2^2}\left(\sum_1^N \left|X_i X_i^{Y}\right| + \sum_1^N \left|Y_i Y_i^{Y}\right|\right)^2 \sum_1^N \left|Z_i Z_i^{Y}\right|}{\frac{1}{3^3}\left(\sum_1^N \left|X_i X_i^{Y}\right| + \sum_1^N \left|Y_i Y_i^{Y}\right| + \sum_1^N \left|Z_i Z_i^{Y}\right|\right)^3} \tag{9}$$

In the following example, two sets of 11 polarimetric images acquired in one month time period are used. The first one was acquired in L band (Figure 10), the second one in UHF band (Figure 11) [21] on an airport area in French Guyana. Both bands were acquired simultaneously. Colour compositions of the 11 images are displayed on the left hand side of the figures. Unchanged areas appear in grey whereas changes are colourful. On the left hand side, the colours correspond to a detected activity (each colour is related to an acquisition date). It is noteworthy to see that the clutter remains stable during one month even at L band and that activity detected at L band corresponds to the one detected at UHF band.

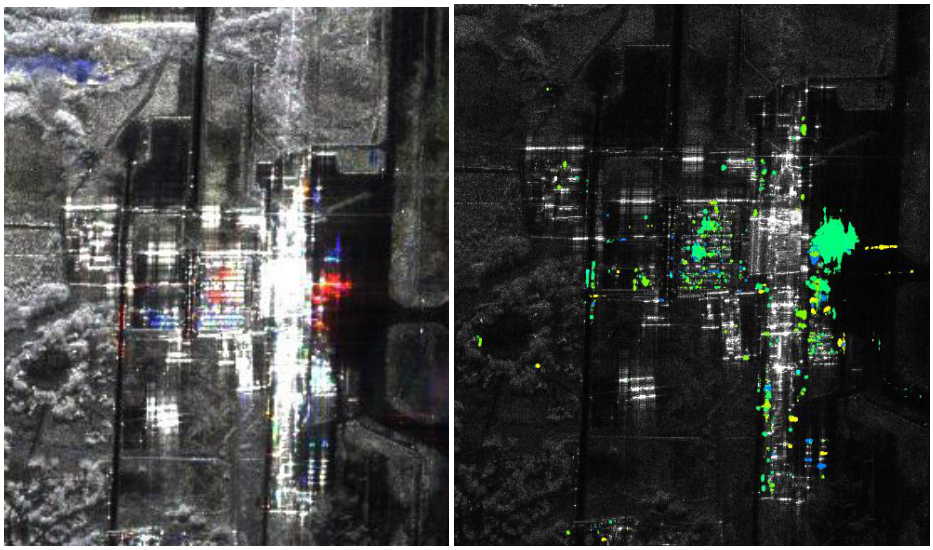

Figure 10: L band colour composite image and detected activity.

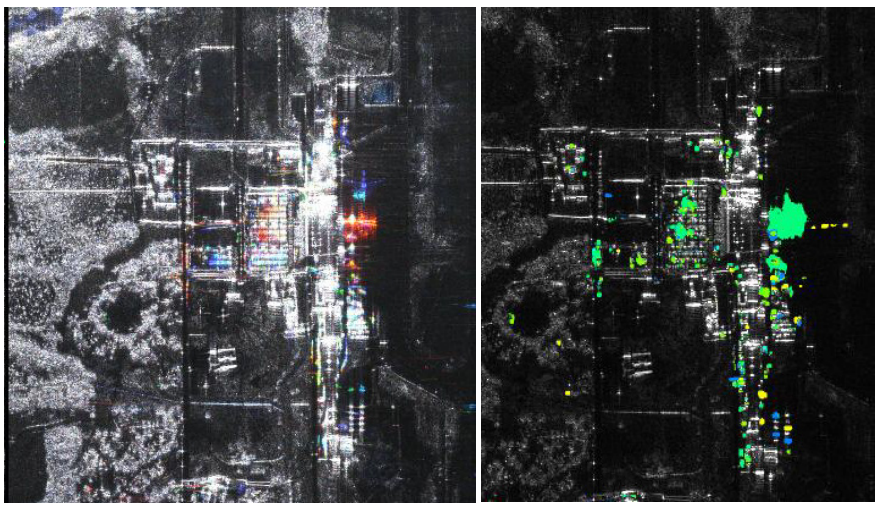

Figure 11: UHF band colour-composite image and detected activity.

7.0 CONLUSION

This paper has shown a diversity of change detection criteria associated with different kinds of images, from UHF images for concealed vehicles detection to very high resolution X band images for tracks detections. It explained that coherent change detection is much more demanding than incoherent change detection in term of similarity of trajectories and coregistration accuracy. Finally examples of change detection have been presented and the applicability of the different methods has been addressed.

8.0 ACKNOWLEDGMENTS

The author wishes to thank the SETHI team for acquiring most of the data presented in this paper.

9.0 REFERENCES

[1] L.M.H. Ulander, M. Lundberg, W. Pierson, A. Gustavsson, "Change detection for low-frequency SAR ground surveillance", *IEE Proc-Radar Sonar Navigation*, Vol 152, n°6, Dec 2005.

[2] K.I. Ranney, "Modified Difference Change Detector for Samll Targets in SAR Imagery", *Aerospace and Electronics Systems, IEEE Transactions on*, vol 44, n°1, pp 57-76, Jan 2008

[3] M. Preiss, D.A. Gray, N.J.S. Stacy "Detecting Scene Changes Using Synthetic Aperture Radar Interferometry", *Geoscience and Remote Sensing, IEEE Transactions on* , vol.44, no.8, pp.2041-2054 , Aug. 2006

[4] S.I. Tsunoda,; Pace, F.; Stence, J.; Woodring, M.; Hensley, W.H.; Doerry, A W.; Walker, B.C., "Lynx: a high-resolution synthetic aperture radar," *Aerospace Conference Proceedings, 2000 IEEE* , vol.5, no., pp.51,58 vol.5, 2000

[5] Y. Bazi, L. Bruzzone, F. Melgani, "An Unsupervised Approach Based on the Generalised Gaussian Model to Automatic Change Detection in Multitemporal SAR Images, *Geoscience and Remote Sensing, IEEE Transactions on* , vol.43, no.4, pp.874-886, Apr. 2005

[6] O. Dogan, D. Perissin, "Detection of Multitransition Abrupt Changes in Multitemporal SAR Images", *Geoscience and Remote Sensing, IEEE Transactions on* , vol accepted for publication,. 2014.

[7] J.W. Goodman, "Some fundamental properties of speckle". *J. Opt. Soc. Am*. n°66 pp 1145–1150, 1977

[8] F. T. Ulaby, and M. C. Dobson, *Handbook of Radar Scattering Statistics for Terrain*, Artech House, Inc., Dedham, Massachusetts, 1989

[9] Chris Oliver, Shaun Quegan, *Understanding Synthetic Aperture Radar Images*, SciTech Publishing, 2004.

[10] F. Gatelli, A. Monti Guarnieri, F. Parizzi, P. Pasquali, C. Prati, F. Rocca, "the wavenumer shift in SAR interferometry", IEEE Transactions on geoscience and remote sensing, vol 32, n°4, july 1994.

[11] R. Bamler, P. Hartl, "Synthetic Aperture Radar Interferometry", *Inverse Problems*, 14, pp. R1-R54, 1998.

[12] K. Papathanassiou and S. Cloude , “Single-baseline polarimetric SAR interferometry,” IEEE Trans. Geosci. Remote Sens., vol. 39, no. 11,pp. 2352–2363, Nov. 2001

[13] Z. Li and J. Bethel "Image coregistration in SAR interferometry", Proc. Int. Arch. Photogramm., Remote Sens. Spatial Inf. Sci., pp.433 -438 2008

[14] M. Preiss, N.J.S. Stacy, "Coherent Change Detection: Theoretical Description and Experimental Results", DSTO-TR-1851, august 2006.

[15] P. Dubois-Fernandez, et al.; "The TropiSAR Airborne Campaign in French Guiana: Objectives, Description, and Observed Temporal Behavior of the Backscatter Signal", *Geoscience and Remote Sensing, IEEE Transactions on* , vol.50, no.8, pp.3228-3241, Aug. 2012

[16] L. Novak, "Algorithms for SAR change Detection Compression and Super-resolution", *Tutorial of Radar conference*; October 2009.

[17] J Inglada, "Change Detection on SAR Images by using a Parametric Estimation of the Kullback-Leibler Divergence", *Geoscience and Remote Sensing Symposium, 2003. IGARSS '03. Proceedings. 2003 IEEE International* , vol.6, no., pp.4104,4106 vol.6, 21-25 July 2003

[18] R. Sabry, "A New Coherency Formalism for Change Detection and Phenomenology in SAR imagery: A filed Approach", *Geoscience and Remote Sensing Letters* , vol.6, no.3, pp.458-462, July 2009

[19] A. Marino, S. Cloude, J. M. Sanchez-Lopez, "A New Polarimetric Change Detector in Radar Imagery", *Geoscience and Remote Sensing, IEEE Transactions on*, vol 51, n°5, pp 2986-3000, 2013.

[20] A. Marino, A; Hajnsek, I, "A Change Detector Based on an Optimization With Polarimetric SAR Imagery," *Geoscience and Remote Sensing, IEEE Transactions on* , vol.52, no.8, pp.4781,4798, Aug. 2014

[21] H. Oriot, W.P. Ang, "activity monitoring in UHF and L band SAR imagery", *Proceedings of Sondra workshop*, june 2013.

[22] H. Oriot, "Change detection analysis for under-cover detection in L and UHF band", *Proceedings of Polinsar Workshop*, jan 2013.

[23] E.J.M. Rignot, J. Van Zyl, "Change Detection Techniques for ERS-1 SAR Data", *Geoscience and Remote Sensing, IEEE Transactions on* , vol.31, no.4, pp.896-906, July 1993